

Dissipation-Induced Heteroclinic Orbits in Tippe Tops

Nawaf Bou-Rabee* Jerrold E. Marsden[†]
Louis A. Romero[‡]

12 February 2008

Abstract

This paper demonstrates that the conditions for the existence of a dissipation-induced heteroclinic orbit between the inverted and noninverted states of a tippe top are determined by a complex version of the equations for a simple harmonic oscillator: the modified Maxwell–Bloch equations. A standard linear analysis reveals that the modified Maxwell–Bloch equations describe the spectral instability of the noninverted state and Liapunov stability of the inverted state. Standard nonlinear analysis based on the energy-momentum method gives necessary and sufficient conditions for the existence of a dissipation-induced connecting orbit between these relative equilibria.

1 Introduction

Tippe tops come in a variety of forms. The most common geometric form is a cylindrical stem attached to a truncated ball, as shown in Figure 1.1. On a flat surface, the tippe top will rest stably with its stem up. However, spun fast enough on its blunt end, the tippe top momentarily defies gravity, inverts,

*Applied and Computational Mathematics, Caltech, Pasadena, CA 91125 (nawaf@acm.caltech.edu). The research of this author was supported by the U.S. DOE Computational Science Graduate Fellowship through grant DE-FG02-97ER25308.

[†]Control and Dynamical Systems, Caltech, Pasadena, CA 91125 (marsden@cds.caltech.edu). The research of this author was partially supported by the National Science Foundation.

[‡]Sandia National Laboratories, P.O. Box 5800, MS 1110, Albuquerque, NM 87185-1110 (lromero@sandia.gov). The research of this author was supported by Sandia National Laboratories. Sandia is a multiprogram laboratory operated by Sandia Corporation, a Lockheed Martin Company, for the United States Department of Energy under contract DE-AC04-94AL85000.

and spins on its stem until dissipation causes it to slow down and then fall over. This spectacular sequence of events occurs because, and in spite of, dissipation.

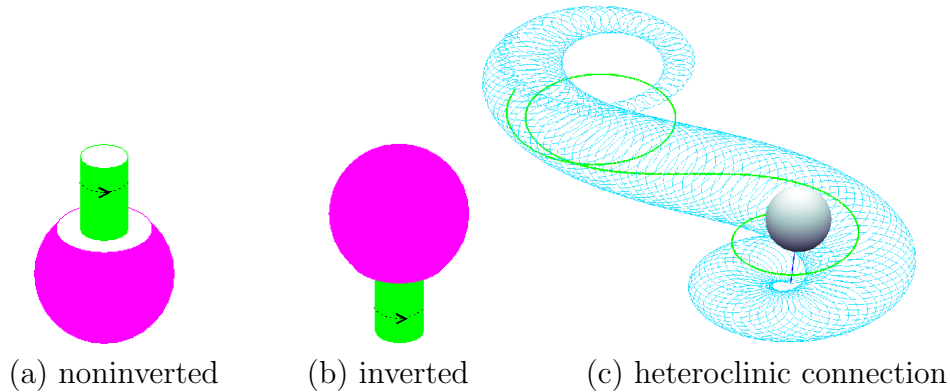


Figure 1.1: **Tippe Top Relative Equilibria & Heteroclinic Orbit.** The noninverted and inverted states of the tippe top, and a still of a numerical simulation of the heteroclinic connection between these states. For movies of numerical simulations with discussion the reader is referred to [5].

Tippe top inversion is a tangible illustration of dissipation-induced instabilities, relative equilibria, and the energy-momentum method. Tippe top inversion can be understood by analyzing a system known as the *modified Maxwell–Bloch equations* [5]. These equations are a complex version of the simple harmonic oscillator and a generalization of a previously derived normal form describing dissipation-induced instabilities in the neighborhood of the 1:1 resonance [16].

Tippe top inversion has been much investigated in the literature. The reader is referred to the works of Cohen [17], Or [33], Ebenfeld and Scheck [18], and Bou-Rabee et al. [5] for surveys of the literature. A key observation made by previous investigators is that one must include friction to model tippe top inversion, and in the limit of zero and infinite friction, tippe top inversion does not occur in the model. In the limit of zero friction, the model tippe top is a holonomic, Hamiltonian system. In the limit of infinite friction, it becomes a nonholonomic, Hamiltonian system [1; 4]. Thus, to analyze tippe top inversion one does not model the system as a nonholonomic Hamiltonian or holonomic Hamiltonian system. Rather, it is modelled as a holonomic, dissipative Hamiltonian system.

Mechanism behind tippe top inversion. The tippe top inverts because it is energetically favorable to do so. This can be made precise in the context of the following mathematical model of a tippe top.

Consider a sphere on a surface with an axisymmetric mass distribution, such that the sphere's center of mass is on its axis of symmetry, but not at its geometric center. The noninverted (inverted) state of the spherical tippe top corresponds to the gravitationally stable (unstable) state in which the sphere is spinning about the vertical direction and the sphere's center of mass is below (above) the geometric center of the sphere. These states model the noninverted and inverted states of a realistic tippe top as depicted in Figures 1.1(a) and 1.1(b). It is assumed that the sphere is in point-contact with the surface, and that the friction the sphere perceives is proportional only to the velocity of this point of contact. As a consequence the noninverted and inverted states of the spherical tippe top become steady-state phenomena, since the contact point is stationary at these states.

Let $\boldsymbol{\pi}$ be the spatial angular momentum of the spherical tippe top and \mathbf{q} the vector connecting its center of mass to the contact point on the surface (cf. Figure 3.1). The *Jellett momentum map* (or Jellett invariant), \mathcal{J} , is defined as

$$\mathcal{J} = -\boldsymbol{\pi} \cdot \mathbf{q}. \quad (1.1)$$

Due to an infinitesimal symmetry of the forces the spherical tippe top perceives with respect to the generator of rotations about \mathbf{q} , \mathcal{J} is conserved along the flow of the tippe top. \mathcal{J} is the momentum map corresponding to rotations about \mathbf{q} on the configuration space of the tippe top. To learn more about momentum maps the reader is referred to [27].

With this conservation law, a simple energy argument intuitively explains tippe top inversion. Consider the two energy states of the tippe top corresponding to the noninverted and inverted states. In the noninverted (inverted) state, the contact vector is alligned to the direction of gravity and has smallest (largest) magnitude. Thus, the gravitational potential energy of the noninverted state is smaller than that of the inverted state.

Yet, assuming \mathcal{J} is some fixed value C , the rotational kinetic energy of the noninverted state is larger than the rotational kinetic energy of the inverted state. This is because in the inverted state the contact vector is longer, and hence, from $\mathcal{J} = C$ the inverted state is spinning slower than the noninverted state. If the initial spin rate is fast enough, this drop in rotational kinetic energy overwhelms the increase in gravitational potential energy. In this case the point which minimizes total energy is the inverted state. This argument is made precise in theorem 5.2; the main result of the paper. This theorem requires some knowledge of dissipation-induced instabilities and heteroclinic orbits, which we review here for the reader's convenience.

Dissipation-Induced Instabilities. In the context of this paper, dissipation is understood as an energy-decreasing nonconservative force. Dissipation plays a key role in enabling the spherical tippe top to access different points on

the Jellett momentum level set. The theory of *dissipation-induced instabilities* provides a mathematical framework to study the effect of dissipation on the stability of Hamiltonian systems. A dissipation-induced instability describes a neutrally stable equilibrium becoming spectrally (and hence Liapunov) unstable with the addition of dissipation. This phenomenon is counter to one's intuition since one expects that dissipation stabilizes neutrally stable equilibria. Yet, dissipation can also play a stabilizing role as evidenced in the spherical tippe top's inversion. To clarify these statements, the following introduction to the theory of dissipation-induced instabilities is provided.

Let $M, G, K \in L(\mathbb{R}^n, \mathbb{R}^n)$ and assume M is a symmetric positive-definite matrix. The setting of the theory of dissipation-induced instabilities is a mechanical system with phase space $T\mathcal{Q} \cong \mathbb{R}^{2n}$ and a quadratic Lagrangian $\mathcal{L} : T\mathcal{Q} \rightarrow \mathbb{R}$ that can be written as:

$$\mathcal{L}(\mathbf{q}, \dot{\mathbf{q}}) = \dot{\mathbf{q}}^T M \dot{\mathbf{q}} + \dot{\mathbf{q}}^T G \mathbf{q} - \mathbf{q}^T K \mathbf{q}$$

For a general, smooth Lagrangian that contains terms of higher than degree two in \mathbf{q} and $\dot{\mathbf{q}}$, a second-order Taylor approximant about some point in $T\mathcal{Q}$ puts its Lagrangian in this form. Since the only conservative forces derivable from a quadratic Lagrangian are gyroscopic and potential, G and K are necessarily skew-symmetric and symmetric matrices respectively. The corresponding Euler-Lagrange equations are given by:

$$M\ddot{\mathbf{q}} + G\dot{\mathbf{q}} + K\mathbf{q} = 0 \tag{1.2}$$

The zero solution of (1.2) is called *potentially unstable* if K has some negative eigenvalues. It is called *potentially stable* if K is positive definite. However, even if the zero solution is potentially unstable, due to G the system can be spectrally (or neutrally) stable. In this case one says that the system is gyroscopically stabilized, since G physically corresponds to gyroscopic effects.

Let $C, V \in L(\mathbb{R}^n, \mathbb{R}^n)$ and assume C is symmetric positive-definite and V is skew-symmetric. If the system is gyroscopically stabilized without friction, counter to our intuition about friction, adding friction proportional to velocities destabilizes the zero-solution of:

$$M\ddot{\mathbf{q}} + C\dot{\mathbf{q}} + G\dot{\mathbf{q}} + K\mathbf{q} = 0. \tag{1.3}$$

However, dissipation is not necessarily a destabilizing force for gyroscopically stabilized systems. In fact, the general theory of dissipation-induced instabilities is concerned with the stability of the zero-solution of the following system:

$$M\ddot{\mathbf{q}} + C\dot{\mathbf{q}} + G\dot{\mathbf{q}} + K\mathbf{q} + V\mathbf{q} = 0 \tag{1.4}$$

where C is symmetric positive-definite and V is skew-symmetric. To model dissipation often one uses dissipation proportional to velocity $C\dot{\mathbf{q}}$ and not

proportional to position $V\mathbf{q}$ or *positional dissipation*. Although the dissipation proportional to velocity is purely destabilizing for a gyroscopically stabilized system, one can obtain stability of a gyroscopically stabilized state if both types of dissipation are present. Also, one can obtain instability of a potentially stable system if both types of dissipation are present.

It makes sense that the spherical tippe top exhibits both of these types of dissipation. Recall the dissipation the top perceives is modelled as friction proportional to the velocity of its point of contact. This type of friction is proportional to the translational velocity of the sphere, the angular velocity of the sphere, and the orientation of the sphere's point of contact. The spinning spherical tippe top exhibits positional dissipation because of the dependence of the friction law used on the orientation of the sphere. In the paper we will show that both types of damping need to be present in order to explain why the spherical tippe top inverts. In this way the spherical tippe top illustrates some important, and not widely known, consequences of the theory of dissipation-induced instabilities.

Dissipation-induced instability theory has a long history, which goes back to Thomson and Tait; see [38]. The central theorems in this area were subsequently proven by Chetayev [14] and extended in the work of Merkin [28] and others. In its modern form, dissipation-induced instability was shown both to be a general phenomenon for gyroscopically stabilized systems and to provide a sharp converse to the energy momentum stability method by Bloch et al. in [2] and [3]. The work of Krechetnikov and Marsden [24] puts this theory into a broader context, including positional forces. The paper [24] also includes a discussion of a number of additional examples, including the well-known follower force problem [13], the Levitron, and radiation-induced instabilities. For a comprehensive history and review of dissipation-induced instabilities, including what is known in the case of PDE and for further references, the reader is referred to [25].

Heteroclinic Orbits. A *heteroclinic orbit* is a path in the phase space of a dynamical system that connects two equilibria. These equilibria need not be static. For example, consider the orbit connecting the inverted and noninverted states of the tippe top. Or, consider the whirling orbit which connects a textbook spun about its unstable intermediate axis to its antipode. These examples motivate the notion of a *relative equilibria* which is equivalent to a fixed point modulo a one-parameter Lie group action. For the tippe top and textbook relative equilibria, this action is an S^1 -rotation about a fixed axis. A *dissipation-induced heteroclinic orbit* is a heteroclinic connection that exists because of (and in spite of) dissipation, as in the tippe top.

Relative equilibria arise frequently in realistic rigid body and fluid systems, and techniques to assess their stability/robustness are in demand. In this paper

we apply the *energy momentum method* to ascertain the existence of a heteroclinic connection. A cornerstone of the method is the energy momentum mapping which we will specify for mechanical systems with phase space P possessing a Lie group G -symmetry. Let \mathfrak{g} and \mathfrak{g}^* be the Lie algebra and dual of the Lie algebra of G . If $\mathcal{E} : P \rightarrow \mathbb{R}$ is the energy of the system, $\mathcal{J} : P \rightarrow \mathfrak{g}^*$ the momentum map associated to the G -symmetry, and \mathcal{J}_e a particular value of this momentum map, the energy momentum map is given by

$$\mathcal{E}_{\mathcal{J}} = \mathcal{E} + \langle \mathcal{J} - \mathcal{J}_e, \lambda \rangle, \quad (1.5)$$

where $\lambda \in \mathfrak{g}$ is a Lagrange multiplier. To establish Liapunov stability by the energy momentum method, one finds critical points of $\mathcal{E}_{\mathcal{J}}$ which correspond to relative equilibria. Then one checks definiteness of the second variation of $\mathcal{E}_{\mathcal{J}}$ at these critical points in directions tangent to the momentum level set (i.e., for all $x \in \ker \mathbf{d}\mathcal{J}$) and transverse to orbits of G . It is a natural tool to invoke in this context given that the Jellett momentum map (cf. (1.1)) is preserved along the flow of tippe tops. For more exposition, applications, and history the reader is referred to [26; 27].

Organization of the Paper. §2 presents the modified Maxwell–Bloch equations and discusses their ability to reproduce tippe top inversion. §3 describes a derivation of the governing equations for the tippe top from a variational principle. §4 casts the linearized equations of the tippe top in the form of modified Maxwell–Bloch equations. §5 contains a standard application of the energy momentum method and LaSalle’s invariance principle to determine necessary and sufficient conditions for existence of a heteroclinic connection between the inverted and noninverted states of the tippe top. §6 provides some concluding remarks on the energy adiabatic momentum method, the curious heteroclinic orbit between the rattleback top’s saddle-like relative equilibria, and related problems.

2 Modified Maxwell–Bloch Equations

This section introduces an important extension of the Maxwell–Bloch equations and studies their stability. These equations are a two-dimensional instance of (1.4). They arise in the study of the linear stability of axisymmetric rigid bodies such as the spherical tippe top.

Derivation. Consider a planar ODE of the form

$$\ddot{q} = f(q, \dot{q}), \quad q = \begin{bmatrix} x \\ y \end{bmatrix}.$$

Linearization of these equations yields

$$\ddot{q} + A\dot{q} + Bq = 0$$

where A and B are 2×2 real matrices. The characteristic polynomial of this system

$$\det \left(\begin{bmatrix} \sigma^2 & 0 \\ 0 & \sigma^2 \end{bmatrix} + A\sigma + B \right) = 0$$

shows that when A is skew-symmetric and B is symmetric the system possesses a spectral symmetry typical of linear Hamiltonian systems, namely if σ is a solution then so are: $\bar{\sigma}$, $1/\sigma$, and $1/\bar{\sigma}$.

We define the rotation matrix

$$R(\theta) = \begin{bmatrix} \cos(\theta) & -\sin(\theta) \\ \sin(\theta) & \cos(\theta) \end{bmatrix}$$

as well as the identity and elementary skew-symmetric matrices in $L(\mathbb{R}^2, \mathbb{R}^2)$ as:

$$I = \begin{bmatrix} 1 & 0 \\ 0 & 1 \end{bmatrix}, \quad S = \begin{bmatrix} 0 & -1 \\ 1 & 0 \end{bmatrix}.$$

The necessary and sufficient condition for a 2×2 matrix to commute with the rotation matrix is that the matrix be a linear combination of I and S . Thus, if this ODE is rotationally symmetric, i.e., the ODE is invariant under $SO(2)$ rotation, then the matrices A and B can be expressed as

$$A = -\alpha S + \beta I, \quad B = -\gamma S + \delta I,$$

where α , β , γ , and δ are real scalars. Because β and γ destroy the spectral symmetry associated to Hamiltonian systems, we call these terms nonconservative.

Given the particular form of the rotationally symmetric ODE, we can write the two-dimensional real system as a one-dimensional complex system,

$$\ddot{z} + i\alpha\dot{z} + \beta\dot{z} + i\gamma z + \delta z = 0, \quad z = x + iy, \tag{2.1}$$

which we call the **modified Maxwell–Bloch equations**. Observe that (2.1) is a complexified version of (1.4) in two dimensions.

Proposition 2.1. *The modified Maxwell–Bloch equations are the linearized normal form for planar, rotationally symmetric dynamical systems.*

(2.1) is the basic harmonic oscillator with the two complex terms $i\alpha\dot{z}$ and $i\gamma z$. In physical systems $i\alpha\dot{z}$ arises from Coriolis effects, and hence is known as the gyroscopic term. Whereas $i\gamma z$ typically arises from dissipation in rotational variables. The damping force $i\gamma z$ is different from the usual damping term

proportional to velocity $\beta\dot{z}$ and will be referred to as complex damping. This type of damping corresponds to the positional dissipation introduced in (1.4). Physically the complex damping term models viscous effects caused by, for example, motion in a fluid, while the usual damping term models internal dissipation.

Before we describe the general stability properties of these equations, let us consider as an illustrative example the stability of a rotating beam. One can show that the linearized equations of the first mode of a rotating beam can be cast in the form of (2.1). In this case α corresponds to the rotation rate of the beam. These linearized equations are the same as the Euler-Lagrange equations for a bead in a rotating circular plate [3]. If one ignores dissipation, the system is potentially stable as long as the rotation rate is less than the resonance frequency of the beam. If the rotation rate is greater than the resonance frequency of the beam, the system becomes gyroscopically stabilized. As mentioned in the introduction, dissipation proportional to velocity destabilizes this gyroscopically stabilized state. Typically damping in a beam is due to internal dissipation which is proportional to velocities, and hence, this explains why one observes a rotating beam become unstable when spun at a rate which exceeds its resonance frequency.

Stability Criteria. The characteristic polynomial of the modified Maxwell–Bloch equations is

$$\lambda^4 + 2\beta\lambda^3 + (\alpha^2 + \beta^2 + 2\delta)\lambda^2 + 2(\alpha\gamma + \beta\delta)\lambda + (\gamma^2 + \delta^2) = 0.$$

We now write the necessary and sufficient conditions for this polynomial to be Hurwitz [19].

Theorem 2.2. *The zero solution of the modified Maxwell–Bloch equations is Liapunov stable iff the following inequalities hold:*

$$\begin{aligned}\beta &> 0, \\ \alpha\beta\gamma - \gamma^2 + \beta^2\delta &> 0, \\ \alpha^2\beta + \beta^3 - \alpha\gamma + \beta\delta &> 0.\end{aligned}$$

The proof of this is a simple application of standard Hurwitz stability criteria as described in, e.g., [19]. There are two especially interesting physical cases of these inequalities:

1. When $\delta > 0$, $\gamma = \beta = 0$, the system is neutrally stable with or without the presence of the gyroscopic term. Adding usual dissipation $\beta\dot{z}$ makes the neutrally stable zero solution Liapunov stable. Adding usual and positional dissipation can stabilize or destabilize the neutrally stable zero solution.

2. When $\delta < 0$, $\alpha > -4\delta > 0$, $\beta = \gamma = 0$, the system is gyroscopically, and hence neutrally, stable. Adding usual dissipation $\beta\dot{z}$ makes the neutrally stable zero solution spectrally unstable since the second inequality in theorem 2.2 can never hold. This case corresponds to the classical dissipation-induced instability [2]. If $\beta = 0$ and $\gamma > 0$, the neutrally stable zero solution becomes spectrally unstable. Adding usual and positional dissipation can stabilize or destabilize the zero solution depending on the ratio of β to γ .

For the tippe top, we will show that dissipation in rotational variables (or complex damping) is essential to understanding inversion. In fact, the remarks above point out some limitations of usual damping: usual damping can only predict instability in the case of a gyroscopically stable system and stability in the case of a gravitationally stable system.

Consider the modified Maxwell–Bloch equations as a possible model of the linearized behavior of the tippe top. In particular, suppose that the noninverted and inverted states of the tippe top correspond to the zero solution of (2.1). Without friction we observe a noninverted state which is gravitationally stable with or without gyroscopic effects. Remark 1 above shows that the addition of usual damping cannot destabilize this gravitationally stable, noninverted state. The complex damping term, however, can destabilize this state. Therefore, the complex damping term can explain why the gravitationally stable tippe top becomes spectrally unstable.

Moreover, after the tippe top inverts we have a gyroscopically stabilized inverted state. We have shown that the addition of usual damping would make such a system spectrally unstable. Thus, usual damping cannot explain why the tippe top spins stably in its inverted state. Remark 2 shows that the complex and usual damping term in the right ratio can, however, stabilize this state. Thus, the complex damping term can also explain why the tippe top spins stably on its stem. We will revisit this analysis when we cast the linearized equations of the tippe top in the form of the modified Maxwell–Bloch equations.

3 Tippe Top Equations

This section contains a pedagogical derivation and analysis of the spherical tippe top's governing equations using a variational principle, given mainly for the reader's convenience. The tippe top is modelled as a sphere in point contact with a surface. At the point of contact, the sphere is subjected to frictional forces tangent to the surface and gravitational forces normal to the surface. The section starts with a derivation of the equations of motion for the system without friction. Friction proportional to the velocity of the point

of contact of the body on the surface is added later. One can also derive these equations using Newtonian mechanics as was done in the earlier version of our paper [5].

In what follows we will often use the hat map to identify a 3×3 skew-symmetric matrix with a vector in \mathbb{R}^3 . Let $\mathfrak{so}(3)$ denote the set of 3×3 skew-symmetric matrices. For a vector $\mathbf{x} = (x_1, x_2, x_3) \in \mathbb{R}^3$, the hat map, $\hat{\cdot} : \mathbb{R}^3 \rightarrow \mathfrak{so}(3)$, is defined as:

$$\widehat{\mathbf{x}} = \begin{bmatrix} 0 & -x_3 & x_2 \\ x_3 & 0 & -x_1 \\ -x_2 & x_1 & 0 \end{bmatrix}.$$

Let $\mathbf{y} = (y_1, y_2, y_3) \in \mathbb{R}^3$. The hat map is related to the cross product in the following way:

$$\widehat{\mathbf{x}}\mathbf{y} = \mathbf{x} \times \mathbf{y}.$$

Mathematical Model. The tippe top is modeled as an axisymmetric rigid body whose external shape is a sphere of radius R and whose mass is M . The sphere is assumed to be in point contact with a fixed plane. Let the points Q , O , and C represent the point of contact, the geometric center, and the center of mass of the sphere, respectively (cf. Figure 3.1). We assume the mass distribution of the sphere is inhomogeneous, but symmetric about an axis through the sphere’s geometric center O . Thus, the sphere’s center of mass C is located on its axis of symmetry $\boldsymbol{\xi}_3$, but at a distance $R\epsilon$ above its geometrical center O where ϵ is the center of mass offset ($0 \leq \epsilon \leq 1$). Let $I_1 = I_2 = I$ and I_3 be the dimensional moment of inertia of the sphere with respect to principal axes attached to C . Since the mass distribution is axisymmetric one can prove that $I_3/I \leq 2$.

Assume that one rescales position by R , time by the gravitational time-scale $\sqrt{R/g}$, and the Lagrangian by Ig/R . Introduce the following dimensionless parameters:

$$\sigma = \frac{I_3}{I}, \quad \text{Fr} = \frac{\Omega^2 R}{g}, \quad \mu = \frac{MR^2}{I}, \quad \nu = c \frac{R^2}{I} \sqrt{\frac{R}{g}},$$

where Ω is the magnitude of the initial angular velocity of the top and c a strictly positive friction factor. The dimensionless parameters σ , Fr , μ , and ν are the inertia ratio, Froude number, dimensionless mass, and friction factor, respectively.

Lagrangian of Tippe Top. The unconstrained configuration space of the tippe top is $\mathcal{Q} = \mathbb{R}^3 \times \text{SO}(3)$ and its unconstrained Lagrangian is denoted $\mathcal{L} : T\mathcal{Q} \rightarrow \mathbb{R}$. Let $(\mathbf{x}(t), \dot{\mathbf{x}}(t)) \in \mathbb{R}^3 \times \mathbb{R}^3$ denote the translational position and

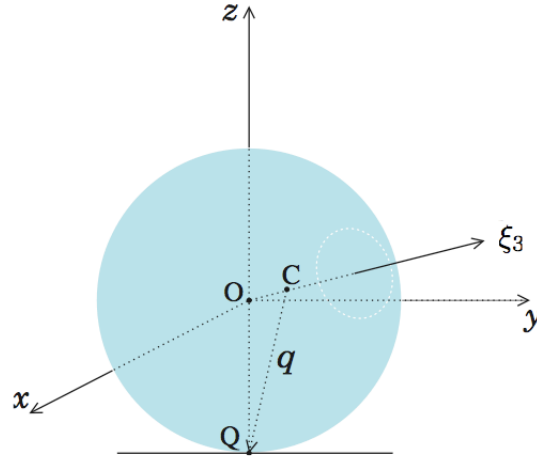


Figure 3.1: **Tippe Top.** We model the tippe top as a sphere with an eccentric center of mass C , geometric center O , and point of contact Q . Vectors \mathbf{q} and $\boldsymbol{\xi}_3$ represent the dimensionless position of the contact point with respect to the center of mass and the unit vector in the direction of the axis of symmetry, respectively.

velocity of the sphere. Let $(\mathbf{R}(t), \boldsymbol{\omega}(t)) \in \text{SO}(3) \times \mathbb{R}^3$ denote the rotational position and spatial angular velocity of the spherical tippe top (where $\mathbf{R}(t)$ is the matrix specifying the orientation of the body). Let $(\mathbf{e}_1, \mathbf{e}_2, \mathbf{e}_3)$ denote an inertial orthonormal frame attached to O and related to a body-fixed frame $(\boldsymbol{\xi}_1, \boldsymbol{\xi}_2, \boldsymbol{\xi}_3)$ attached to O by the formulae:

$$\mathbf{R}\mathbf{e}_i = \boldsymbol{\xi}_i, \quad i = 1, 2, 3.$$

In the analysis the vectors \mathbf{e}_3 and $\boldsymbol{\xi}_3$ play an important role, and correspond to unit vectors in the vertical direction and in the direction of the axis of symmetry of the sphere, respectively. Let $\mathbb{I} = \text{diag}(1, 1, \sigma)$ be the standard (dimensionless) diagonal inertia matrix of the body.

We will use the isomorphism between \mathbb{R}^3 and the Lie algebra of $\text{SO}(3)$, $\mathfrak{so}(3)$, given by the hat map. In terms of this identification, the left-trivialized Lagrangian $\ell : \mathbb{R}^3 \times \mathbb{R}^3 \times \text{SO}(3) \times \mathbb{R}^3 \rightarrow \mathbb{R}$ is defined as

$$\ell(\mathbf{x}, \dot{\mathbf{x}}, \mathbf{R}, \boldsymbol{\omega}) = \mathcal{L}(\mathbf{x}, \dot{\mathbf{x}}, \mathbf{R}, \widehat{\boldsymbol{\omega}}\mathbf{R}).$$

For the tippe top, this is simply a sum of the translational kinetic energy, rotational kinetic energy and gravitational potential energy of the sphere

$$\ell(\mathbf{x}, \dot{\mathbf{x}}, \mathbf{R}, \boldsymbol{\omega}) = \underbrace{\frac{\mu}{2} \dot{\mathbf{x}}^T \dot{\mathbf{x}}}_{\text{translational kinetic energy}} + \underbrace{\frac{1}{2} \boldsymbol{\omega}^T \boldsymbol{\omega} + \frac{1}{2} (\sigma - 1) (\boldsymbol{\omega}^T \boldsymbol{\xi}_3)^2}_{\text{rotational kinetic energy}} + \underbrace{-\mu \mathbf{x}^T \mathbf{e}_3}_{\text{gravitational potential energy}} \tag{3.1}$$

The dimensionless position of the contact point relative to the center of mass is given by,

$$\mathbf{q} = -\mathbf{e}_3 - \epsilon \boldsymbol{\xi}_3. \tag{3.2}$$

The sphere is subject to a holonomic constraint $\varphi : \mathbb{R}^3 \times \text{SO}(3) \rightarrow \mathbb{R}$ given by:

$$\varphi(\mathbf{x}, \mathbf{R}) = -1 - \epsilon \boldsymbol{\xi}_3^T \mathbf{e}_3 + \mathbf{e}_3^T \mathbf{x} = \mathbf{q}^T \mathbf{e}_3 + \mathbf{e}_3^T \mathbf{x} = 0. \tag{3.3}$$

Notice that this constraint depends on both the translational and rotational positions of the sphere. Physically it states that the sphere is in point-contact with the surface whose normal is given by the unit vector \mathbf{e}_3 . This vector is opposite the direction of gravity.

Governing Conservative Equations. The phenomenon of interest, tippe top inversion, needs to include friction, but for simplicity we will start by examining the governing equations without friction. The equations of motion will be determined using a Hamilton-Pontryagin description of rigid-body-type systems [7]. This principle unifies the Hamiltonian and Lagrangian descriptions of mechanics. The constrained HP action integral is given by,

$$s = \int_0^t \left[\ell(\mathbf{x}, \mathbf{v}, \mathbf{R}, \boldsymbol{\omega}) + \langle \mathbf{p}, \dot{\mathbf{x}} - \mathbf{v} \rangle + \langle \hat{\boldsymbol{\pi}}, \dot{\mathbf{R}}\mathbf{R}^T - \hat{\boldsymbol{\omega}} \rangle + \lambda \varphi(\mathbf{x}, \mathbf{R}) \right] dt.$$

Observe that this principle enlarges the domain of the classical action by treating the kinematic relations as constraints. The associated Lagrange multipliers \mathbf{p} and $\boldsymbol{\pi}$ are the translational and spatial angular momenta respectively.

The HP principle states that

$$\delta s = 0$$

where the variations are arbitrary except that the endpoints $(\mathbf{x}(0), \mathbf{R}(0))$ and $(\mathbf{x}(T), \mathbf{R}(T))$ are held fixed. A critical point of s satisfies:

$$\left\{ \begin{array}{l} \dot{\mathbf{x}} = \mathbf{v}, \\ \mu \dot{\mathbf{v}} = (\lambda - \mu) \mathbf{e}_3, \\ \mathbf{x}^T \mathbf{e}_3 = 1 + \epsilon \mathbf{e}_3^T \boldsymbol{\xi}_3, \\ \dot{\mathbf{R}} = \hat{\boldsymbol{\omega}} \mathbf{R}, \\ \dot{\boldsymbol{\pi}} = -\lambda \epsilon \boldsymbol{\xi}_3 \times \mathbf{e}_3, \\ \boldsymbol{\pi} = \boldsymbol{\omega} + (\sigma - 1) (\boldsymbol{\omega}^T \boldsymbol{\xi}_3) \boldsymbol{\xi}_3. \end{array} \right. \tag{3.4}$$

These equations are a differential algebraic system in terms of the fixed unit vector \mathbf{e}_3 (corresponding to the normal to the surface) and the following unknowns: the sphere's translational position $\mathbf{x}(t)$, translational velocity $\mathbf{v}(t)$,

rotational position $\mathbf{R}(t)$ (the matrix specifying the orientation of the sphere), spatial angular velocity $\boldsymbol{\omega}(t)$ and spatial angular momentum $\boldsymbol{\pi}(t)$.

Physically the set of equations in (3.4) make much sense. The first and fourth equations are kinematic constraints relating the translational and spatial angular velocity of the sphere to the translational and rotational positions, respectively. The second equation is a balance of linear momentum and shows that the only forces acting on the body are due to gravity and the surface's normal reaction force which are proportional to μ and λ , respectively. The third equation is the constraint that specifies that the sphere is in point-contact with the surface. The fifth equation is a balance of angular momentum and shows that the only torque acting on the body is due to the normal reaction force. The sixth equation relates the spatial angular momentum to the spatial angular velocity of the spherical tippe top.

Recall, the unit vector in the direction of the axis of symmetry is the third column of the rotation matrix, i.e., $\boldsymbol{\xi}_3(t) = \mathbf{R}(t)\mathbf{e}_3$. One can eliminate $\boldsymbol{\omega}$ and λ to obtain a Cauchy problem which has a well-defined flow. Moreover, as a consequence of axisymmetry, one does not need to solve for the evolution of all three columns of $\mathbf{R}(t)$ to integrate the ODE in $\boldsymbol{\pi}$. Instead one just needs to solve for the evolution of the third column, $\boldsymbol{\xi}_3$, using:

$$\dot{\boldsymbol{\xi}}_3 = \boldsymbol{\omega} \times \boldsymbol{\xi}_3. \tag{3.5}$$

From analyzing (3.4) one can deduce that there are two independent quantities which are conserved under its flow as described in the following theorem.

Theorem 3.1. *Let a, b be any real numbers. The following momentum map is conserved under the flow of (3.4),*

$$J = a\boldsymbol{\pi}^T\boldsymbol{\xi}_3 + b\boldsymbol{\pi}^T\mathbf{e}_3.$$

Proof. One can deduce this conservation law from the variational principle as a symmetry of the left-trivialized Lagrangian, i.e.,

$$\ell(\mathbf{x}, \dot{\mathbf{x}}, \mathbf{R}, \boldsymbol{\omega}) = \ell(\mathbf{x}, \dot{\mathbf{x}}, \mathbf{BR}, \mathbf{B}\boldsymbol{\omega})$$

for any $\mathbf{B} \in \text{SO}(3)$ that is a rotation about $\boldsymbol{\xi}_3$ and/or \mathbf{e}_3 . Note that tacit in this argument is that this symmetry action leaves the holonomic constraint invariant. Alternatively, one can deduce this conservation law directly from the equations:

$$\frac{d}{dt}J = a\dot{\boldsymbol{\pi}}^T\boldsymbol{\xi}_3 + a\boldsymbol{\pi}^T\dot{\boldsymbol{\xi}}_3 + b\dot{\boldsymbol{\pi}}^T\mathbf{e}_3$$

From the fifth equation in (3.4), the first and third term in the above vanish. From (3.5) and the sixth equation in (3.4), the second term in the above vanishes. ■

This conservation law indicates that if initially the tippe top is spinning in a neighborhood of its noninverted state (i.e., $\boldsymbol{\xi}_3(0) \approx -\mathbf{e}_3$, $\boldsymbol{\pi}(0) \approx \sigma \text{Fr} \mathbf{e}_3$), then inversion, i.e., the existence of some time T such that $\boldsymbol{\xi}_3(T) \approx \mathbf{e}_3$, cannot occur. Thus, one cannot obtain tippe top inversion by gyroscopic and gravitational effects alone. This result suggests surface friction plays a crucial role in producing this phenomenon.

Governing Nonconservative Equations. Let $\mathbf{q} = -\mathbf{e}_3 - \epsilon \boldsymbol{\xi}_3$ denote the vector connecting the center of mass C to the contact point Q as shown in Fig. 3.1. We model the surface frictional force using a sliding friction law proportional to the velocity of the point of contact of the spherical tippe top:

$$\mathbf{V}_Q = \dot{\mathbf{x}} + \boldsymbol{\omega} \times \mathbf{q}. \tag{3.6}$$

The force and torque due to friction are therefore,

$$\mathbf{F}_f = -\nu \mathbf{V}_Q, \quad \mathbf{M}_f = \mathbf{q} \times \mathbf{F}_f$$

where ν is the dimensionless friction factor. The governing dynamical equations of the spherical tippe top with friction are given by:

$$\left\{ \begin{array}{l} \dot{\mathbf{x}} = \mathbf{v}, \\ \mu \dot{\mathbf{v}} = (\lambda - \mu) \mathbf{e}_3 + \mathbf{F}_f, \\ \mathbf{x}^T \mathbf{e}_3 = 1 + \epsilon \mathbf{e}_3^T \boldsymbol{\xi}_3, \\ \dot{\boldsymbol{\xi}}_3 = \boldsymbol{\omega} \times \boldsymbol{\xi}_3, \\ \dot{\boldsymbol{\pi}} = -\lambda \epsilon \boldsymbol{\xi}_3 \times \mathbf{e}_3 + \mathbf{q} \times (\mathbf{F}_f), \\ \boldsymbol{\pi} = \boldsymbol{\omega} + (\sigma - 1) (\boldsymbol{\omega}^T \boldsymbol{\xi}_3) \boldsymbol{\xi}_3. \end{array} \right. \tag{3.7}$$

These equations are a differential algebraic system in terms of the sphere’s translational position $\mathbf{x}(t)$, translational velocity $\mathbf{v}(t)$, axis of symmetry $\boldsymbol{\xi}_3$, angular velocity $\boldsymbol{\omega}(t)$ and angular momentum $\boldsymbol{\pi}(t)$. These equations can be derived from a Lagrange d’Alembert principle [27]. This principle simply appends the work done by the frictional force and its torque to the Hamilton-Pontryagin principle. The principle is explicitly given by:

$$\delta s + \int_0^t \mathbf{F}_f^T \delta \mathbf{x} dt + \int_0^t \mathbf{M}_f^T \boldsymbol{\eta} dt = 0$$

where $\widehat{\boldsymbol{\eta}} = \delta \mathbf{R} \mathbf{R}^T$. With dissipation the symmetry that led to theorem 3.1 is broken, but not completely. By an infinitesimal symmetry of the forces with respect to the generator of rotations about the contact vector \mathbf{q} , the **Jellett momentum map** is preserved. This infinitesimal symmetry does not depend on the precise form of \mathbf{F}_f , but only that its moment \mathbf{M}_f is orthogonal to \mathbf{q} .

Theorem 3.2 (Jellett Momentum Map). *The following momentum map is conserved under the flow of (3.7),*

$$\mathcal{J} = \boldsymbol{\pi}^T \boldsymbol{\xi}_3 + \epsilon \boldsymbol{\pi}^T \mathbf{e}_3.$$

or $\mathcal{J} = -\boldsymbol{\pi}^T \mathbf{q}$.

Proof. This proof is terse. From (3.7) it follows that

$$\frac{d}{dt} \mathcal{J} = \dot{\boldsymbol{\pi}}^T \mathbf{q} + \boldsymbol{\pi}^T \dot{\mathbf{q}}$$

From the fifth equation in (3.7), the first term vanishes. The second term can be written as:

$$\boldsymbol{\pi}^T \dot{\mathbf{q}} = \epsilon \boldsymbol{\pi}^T \dot{\boldsymbol{\xi}}_3.$$

From the proof of theorem 3.1, this term vanishes as well. ■

This property of the flow of (3.7) simplifies the analysis of tippe top inversion, since it implies that even with dissipation the system evolves on a level set of \mathcal{J} .

Equilibria. In the coordinates we have chosen to write down (3.7) the inverted and noninverted states of the spherical tippe top as illustrated in Fig. 1.1 (relative equilibria) are fixed points of the equations of motion. In particular, all fixed points of (3.7) are translationally stationary and satisfy:

$$\begin{aligned} \dot{\boldsymbol{\xi}}_3 = 0 &\implies \boldsymbol{\xi}_3 \text{ and } \boldsymbol{\omega} \text{ are collinear,} \\ \dot{\boldsymbol{\pi}} = 0 &\implies \boldsymbol{\xi}_3 \text{ and } \mathbf{e}_3 \text{ are collinear.} \end{aligned}$$

At fixed points the Lagrange multiplier satisfies $\lambda = \mu$.

If one restricts to a level set of \mathcal{J} , there are only two fixed points of the equations. Set one of these fixed points to be the noninverted state defined by

$$\boldsymbol{\pi}^1 = \sigma \text{Fr} \mathbf{e}_3, \quad \boldsymbol{\xi}_3^1 = -\mathbf{e}_3, \tag{3.8}$$

which implies $\mathcal{J} = \sigma \text{Fr}(1 - \epsilon)$. The second fixed point on this level set of \mathcal{J} corresponds to the inverted state and satisfies:

$$\boldsymbol{\pi}^2 = \sigma \text{Fr} \frac{1 - \epsilon}{1 + \epsilon} \mathbf{e}_3, \quad \boldsymbol{\xi}_3^2 = \mathbf{e}_3. \tag{3.9}$$

4 Tippe Top Modified Maxwell–Bloch

For this section we will assume translation of the center of mass is negligible. This assumption greatly simplifies the equations. Later we will confirm that the stability criteria derived in this fashion agree with a nonlinear stability analysis, and in particular, we will show that the position of the spherical tippe top’s center of mass remains fixed at all extrema of the energy-momentum map. Ignoring translational effects and eliminating $\boldsymbol{\omega}$ in (3.7) one obtains the following fully nonlinear rotational equations for the spherical tippe top:

$$\begin{cases} \dot{\boldsymbol{\xi}}_3 &= \boldsymbol{\pi} \times \boldsymbol{\xi}_3, \\ \dot{\boldsymbol{\pi}} &= -\mu\epsilon\boldsymbol{\xi}_3 \times \mathbf{e}_3 + \nu\mathbf{q} \times \mathbf{q} \times \boldsymbol{\pi} - \nu\frac{\sigma-1}{\sigma}(\boldsymbol{\pi}^T\boldsymbol{\xi}_3)\mathbf{q} \times \mathbf{q} \times \boldsymbol{\xi}_3. \end{cases} \quad (4.1)$$

Notice that these are a set of differential equations in the unit vector in the direction of the axis of symmetry $\boldsymbol{\xi}_3(t) \in \mathbb{R}^3$ and the spatial angular momentum of the spherical tippe top $\boldsymbol{\pi}(t) \in \mathbb{R}^3$. In these equations \mathbf{e}_3 is a constant vector and \mathbf{q} is as defined in (3.2). As mentioned in the introduction, (4.1) possesses dissipation proportional to velocity and position since the friction law used is a function of both the angular velocity of the sphere and the contact vector \mathbf{q} . As can be easily checked, (4.1) has the following fixed points:

$$\boldsymbol{\pi} = \pi_0\mathbf{e}_3, \quad \boldsymbol{\xi}_3 = n_0\mathbf{e}_3, \quad n_0^2 = 1. \quad (4.2)$$

Set $\boldsymbol{\Phi} = \boldsymbol{\xi}_3^T\mathbf{e}_1 + i\boldsymbol{\xi}_3^T\mathbf{e}_2$. Linearizing (4.1) about (4.2) gives the tippe top modified Maxwell-Bloch equations:

$$\ddot{\boldsymbol{\Phi}} + ia\dot{\boldsymbol{\Phi}} + b\dot{\boldsymbol{\Phi}} + ic\boldsymbol{\Phi} + d\boldsymbol{\Phi} = 0, \quad (4.3)$$

where

$$a = \pi_0, \quad b = \nu(1 + n_0\epsilon)^2, \quad c = \pi_0\nu(1 + n_0\epsilon)/\sigma, \quad d = -\epsilon\mu n_0.$$

Using the stability criteria for modified Maxwell–Bloch systems (cf. theorem 2.2), one can readily deduce the following.

Theorem 4.1. *Consider the relative equilibria defined by (3.8) and (3.9) on the level set $\mathcal{J} = \sigma Fr(1 - \epsilon)$. The noninverted state ($n_0 = -1, \pi_0 = \sigma Fr$) is Liapunov stable iff*

$$\epsilon\mu(1 - \epsilon)^2 + Fr^2(\sigma(1 - \epsilon) - 1) > 0.$$

The inverted state ($n_0 = 1, \pi_0 = \sigma Fr\frac{1-\epsilon}{1+\epsilon}$) is Liapunov stable iff

$$-\epsilon\mu(1 + \epsilon)^4 + Fr^2(1 - \epsilon)^2(\sigma(1 + \epsilon) - 1) > 0.$$

Proof. Assume ν is strictly positive. By theorem 2.2 the noninverted state ($n_0 = -1, \pi_0 = \sigma \text{Fr}$) is stable iff

$$\begin{cases} \epsilon\mu(1 - \epsilon)^2 + \text{Fr}^2(\sigma(1 - \epsilon) - 1) > 0, \\ \epsilon\mu(1 - \epsilon) + (1 - \epsilon)^5\nu^2 - \text{Fr}^2\sigma + \text{Fr}^2\sigma^2(1 - \epsilon) > 0. \end{cases} \quad (4.4)$$

Likewise, the inverted state ($n_0 = 1, \pi_0 = \sigma \text{Fr} \frac{1-\epsilon}{1+\epsilon}$) is stable iff

$$\begin{cases} -\epsilon\mu(1 + \epsilon)^4 + \text{Fr}^2(1 - \epsilon)^2(\sigma(1 + \epsilon) - 1) > 0, \\ -\epsilon\mu(1 + \epsilon)^2 + (1 + \epsilon)^6\nu^2 - \frac{\text{Fr}^2(1-\epsilon)^2\sigma}{1+\epsilon} + \text{Fr}^2(1 - \epsilon)^2\sigma^2 > 0. \end{cases} \quad (4.5)$$

It is easy to confirm that if the first inequalities in (4.4) and (4.5) hold then the second inequalities hold. ■

Observe that this stability criteria is independent of the magnitude of the dimensionless friction factor ν . Can we reduce (4.3) any further? The answer is no because of the remarks made in §2. In particular, it can be shown that, without the usual and complex damping terms, i.e., $b = 0$ and $c = 0$ or $\nu = 0$, the gravitationally stable noninverted state cannot become spectrally unstable. Moreover, the gyroscopically stabilized state can be Liapunov stable if and only if the complex and usual damping terms are present and in the right ratio.

5 Heteroclinic Orbit

The following nonlinear analysis for the tippe top is standard and based on the energy-momentum method for mechanical systems with symmetry [27]. We note that a similar global connecting argument was provided in [22].

To establish the existence of a heteroclinic orbit that describes tippe top inversion, we will invoke LaSalle’s principle [1]. Consider a vector field χ on a manifold P . Let V be a Lyapunov function with negative semidefinite orbital derivative: $V_t \leq 0$ for all $z \in P$. We define the set $\aleph := \{z \in P | V_t(z) = 0\}$.

Theorem 5.1 (LaSalle’s principle). *Let $z : [0, \infty) \rightarrow P$ be an integral curve of a vector field χ with initial condition $z(0) = z_0$. Suppose there is a positively invariant set (trapping region) M such that $z(t) \in M$ for all $t \geq 0$. Then $z(t)$ converges to the largest subset of $\aleph \cap M$ that is invariant under the flow of χ for all t , positive and negative.*

The energy of the tippe top is a natural candidate for a Lyapunov function,

$$\mathcal{E} = \frac{\mu}{2} \mathbf{v}^T \mathbf{v} + \frac{1}{2} \boldsymbol{\pi}^T \boldsymbol{\pi} - \frac{1}{2} \frac{(\sigma - 1)}{\sigma} (\boldsymbol{\pi}^T \boldsymbol{\xi}_3)^2 + \mu \mathbf{x}^T \mathbf{e}_3. \quad (5.1)$$

It is a sum of translational, rotational, and gravitational components. It’s orbital derivative along the flow of (3.7) is given by

$$\frac{d}{dt} \mathcal{E} = -\nu \|\mathbf{V}_Q\|^2, \quad (5.2)$$

where $\|\mathbf{V}_Q\|$ is the magnitude of the slip velocity. Integrating yields,

$$\mathcal{E}(t) = \mathcal{E}(0) - \int_0^t \nu \|\mathbf{V}_Q\|^2 ds.$$

Observe that the energy decreases monotonically until it belongs to a set of states of no-slip friction defining \aleph , and according to LaSalle’s principle, reaches a trapping region within this set.

Let T^*S denoted the constrained phase space of the tippe top. Let $\mathcal{J}_e = \sigma Fr(1 - \epsilon)$ be the value of the Jellett momentum map for (3.8). Define the **energy-Jellett momentum map**, $\mathcal{E}_{\mathcal{J}} : T^*S \times \mathbb{R} \rightarrow \mathbb{R}$ as,

$$\mathcal{E}_{\mathcal{J}} = \mathcal{E} + \lambda (\mathcal{J} - \mathcal{J}_e). \tag{5.3}$$

Label the relative equilibria defined by (3.8) and (3.9) as z_i and z_f , respectively. It is easy to show that there exist Lagrange multipliers, $\lambda_i, \lambda_f \in \mathbb{R}$, such that (z_i, λ_i) and (z_f, λ_f) are critical points of $\mathcal{E}_{\mathcal{J}}$, i.e.,

$$d\mathcal{E}_{\mathcal{J}}(z_i, \lambda_i) = d\mathcal{E}_{\mathcal{J}}(z_f, \lambda_f) = 0. \tag{5.4}$$

In the following theorem, a heteroclinic orbit between these states is determined by LaSalle’s principle and analyzing the critical points of $\mathcal{E}_{\mathcal{J}}$.

Theorem 5.2 (Dissipation-Induced Heteroclinic Orbit). *Label the relative equilibria on the level set $\mathcal{J} = \sigma Fr(1 - \epsilon)$ defined by (3.8) and (3.9) as z_i and z_f , respectively. These relative equilibria are globally connected iff the inverted state is Liapunov stable and the noninverted state is spectrally unstable.*

This theorem is based on finding conditions for which z_i and z_f define the only critical points of $\mathcal{E}_{\mathcal{J}}$. These conditions turn out to satisfied when z_i is spectrally unstable and z_f is Liapunov stable (cf. theorem 4.1). By LaSalle’s principle the trapping region of the Liapunov stable point z_f is accessed as it is the only such set in \aleph .

Lemma 5.3 (Tippe Top Relative Equilibria). *The noninverted and inverted states of the tippe top and their associated Lagrange multipliers, (z_i, λ_i) and (z_f, λ_f) , are the only critical points of $\mathcal{E}_{\mathcal{J}}$ if and only if:*

$$\begin{cases} -\epsilon\mu(1 - \epsilon)^2 - Fr^2(\sigma(1 - \epsilon) - 1) > 0, \\ -\epsilon\mu(1 + \epsilon)^4 + Fr^2(1 - \epsilon)^2(\sigma(1 + \epsilon) - 1) > 0. \end{cases} \tag{5.5}$$

Proof. As a first step, we write $\mathcal{E}_{\mathcal{J}}$ as an unconstrained function and introduce additional Lagrange multipliers to constrain to T^*S . For this purpose let $E : \mathbb{R}^{12} \rightarrow \mathbb{R}$ and $J : \mathbb{R}^{12} \rightarrow \mathbb{R}$ be the unconstrained energy and Jellett momentum map respectively. Let $E_J : \mathbb{R}^{12} \rightarrow \mathbb{R}$ denote the unconstrained energy momentum map which satisfies $\mathcal{E}_{\mathcal{J}} = E_J|_{T^*S}$. Let $\phi : \mathbb{R}^6 \rightarrow \mathbb{R}$ denote the unconstrained version of (3.3) defined as:

$$\phi(\mathbf{x}, \boldsymbol{\xi}_3) = \mathbf{x}^T \mathbf{e}_3 - 1 - \epsilon \boldsymbol{\xi}_3^T \mathbf{e}_3.$$

Consider the map $f : \mathbb{R}^{15} \rightarrow \mathbb{R}$ defined by

$$f = E + \lambda_1(J - \mathcal{J}_e) + \lambda_2\phi + \lambda_3(\|\boldsymbol{\xi}_3\|^2 - 1).$$

The Lagrange multipliers simultaneously constrain the critical point of the energy to a level set of J , constrain $\boldsymbol{\xi}_3$ to S^2 , and ensure the surface constraint is satisfied. A critical point of f satisfies:

$$\mathbf{d}f(\mathbf{x}, \mathbf{v}, \boldsymbol{\xi}_3, \boldsymbol{\pi}, \lambda_1, \lambda_2, \lambda_3) = 0.$$

By direct calculation one can show that these critical points satisfy,

$$\lambda_2 = -\mu, \quad \mathbf{v} = 0$$

and a system of five equations in the five unknowns

$$\lambda_1, \quad \lambda_3, \quad \boldsymbol{\pi}^T \mathbf{e}_3, \quad \boldsymbol{\pi}^T \boldsymbol{\xi}_3, \quad \text{and} \quad \boldsymbol{\xi}_3^T \mathbf{e}_3,$$

with the condition that $(\boldsymbol{\xi}_3^T \mathbf{e}_3)^2 \leq 1$. If \mathbf{e}_3 and $\boldsymbol{\xi}_3$ are collinear these critical points are defined by z_i and z_f . However, if \mathbf{e}_3 and $\boldsymbol{\xi}_3$ are linearly independent then $(\boldsymbol{\xi}_3^T \mathbf{e}_3)^2 < 1$ and one can show that critical points are determined by the zeros of the following polynomial function in $n = \boldsymbol{\xi}_3^T \mathbf{e}_3$:

$$g(n) = \text{Fr}^2(1 - \epsilon)^2 \sigma^2 (n(-1 + \sigma) + \epsilon\sigma) - \epsilon\mu(1 - n^2 + (n + \epsilon)^2 \sigma)^2. \quad (5.6)$$

Observe that (5.5) implies that:

$$\begin{aligned} g(-1) &= -\sigma^2(1 - \epsilon)^2 (\text{Fr}^2(\sigma(1 - \epsilon) - 1) + \epsilon\mu(1 - \epsilon)^2) > 0, \\ g(1) &= \sigma^2 (\text{Fr}^2(1 - \epsilon)^2(\sigma(1 + \epsilon) - 1) - \epsilon\mu(1 + \epsilon)^4) > 0. \end{aligned}$$

The following argument shows that (5.5) implies there are no solutions to $g(n) = 0$ for σ strictly positive. If $\sigma = 1$ it is easy to show that there are no solutions to $g(n) = 0$ such that $|n| < 1$. If $\sigma > 1$ then by convexity it is easy to see that:

$$\text{Fr}^2(1 - \epsilon)^2 \sigma^2 (n(\sigma - 1) + \epsilon\sigma) > \epsilon\mu(1 - n^2 + (n + \epsilon)^2 \sigma)^2 \quad \text{for} \quad n \in [-1, 1].$$

If $\sigma < 1$, the maximum of $1 - n^2 + (n + \epsilon)^2\sigma$ occurs at $n^* = \epsilon\sigma/(1 - \sigma)$. However, if $n^* \leq 1$ then the term $\epsilon\sigma - n(1 - \sigma)$ vanishes and (5.5) does not hold. If $n^* > 1$, then it is easy to see that

$$\text{Fr}^2(1 - \epsilon)^2\sigma^2(-n(1 - \sigma) + \epsilon\sigma) > \epsilon\mu(1 - n^2 + (n + \epsilon)^2\sigma)^2 \quad \text{for } n \in [-1, 1].$$

since the RHS in the above inequality is monotonically increasing for $n \in [-1, 1]$. And hence, z_i and z_f define the unique critical points if and only if (5.5) is satisfied. ■

To use lemma 5.3 to prove theorem 5.2, one can invoke theorem 4.1 or check definiteness of the Hessian of $\mathcal{E}_{\mathcal{J}}$ in directions tangent to the level set of \mathcal{J} and transverse to rotations about \mathbf{q} . This check shows that z_i is an energetic saddle and z_f is an energetic minimum.

For a stability analysis of intermediate relative equilibria, i.e., those for which the tippe top does not fully invert, the reader is referred to [39; 15].

6 Concluding Remarks

We conclude with a few remarks on related mechanical systems as well as related stability issues. The reader is directed to the July 13, 2007 New Scientist Short Sharp Science blog for a video of Tadashi Tokieda (Cambridge University) explaining the curious behavior of other mechanical “toys” including the rattleback top discussed below.

Energy Adiabatic Momentum Method. In the paper [6], we extend the energy momentum method to situations where an adiabatic momentum map exists on a certain time-scale and apply it to the “rising egg” phenomena. We assume this adiabatic momentum map corresponds to an approximate symmetry of the mechanical system. This situation arises, e.g., when one adds ellipticity to the tippe top to analyze the rising of an egg, or more generally, the rising of tops [30; 31; 6]. The Jellett momentum map in this context is no longer an exact invariant.

However, under a fast top approximation, the Jellett momentum map is an adiabatic invariant in rising egg motion as discovered in [30]. The procedure to prove this is a standard application of averaging which introduces an S^1 symmetry corresponding to the symmetry of the Jellett momentum map. The presence of this adiabatic invariant simplifies the analysis of a dissipation-induced heteroclinic orbit connecting the nonrisen to risen state of a rising top. In [6] it is shown that under a fast top approximation, $\epsilon \ll 1$, (where ϵ can be thought of as being inversely related to the spin rate) this momentum is constant with $O(\epsilon^2)$ error on the time-scale t/ϵ . Since the spheroid rises only if the spin is fast enough, this fast-top approximation is appropriate.

Using a multiscale analysis, Moffatt et al. [32] theoretically predict a fascinating transient instability in rising egg motion that manifests itself in the egg jumping on a time-scale that is fast compared to the time-scale associated to rising. Interestingly, Mitsui et al. [29] confirm this finding experimentally! The authors use a sophisticated apparatus that mechanically spins a spheroid at high speeds and simultaneously measures optical, acoustic and electric signals generated by it.

Dynamic Stability by Time-Periodic Forcing. Time-periodic excitations in mechanical systems lead to surprising phenomena. The fact that under the action of vibrations, the inverted position of the pendulum can become stable by time-periodically exciting its suspension point is a classical example [23]. Or, as discovered by Wolfgang Paul, one can also use time-periodic electric fields to confine charged particles [34]. Yet another example involves a coupling of electromagnetic and gyroscopic effects to achieve so-called spin-stabilized magnetic levitation; see, e.g., [35; 36] and references therein.

As a final example we consider the action of vibrations on a *complex fluid* as shown in Fig. 6.1. The following dynamics is observed. Initially, the free surface of an aqueous suspension of cornstarch in a container is flat. Under the action of vibrations, the fluid can permanently support holes and vertical fingerlike protrusions through its surface appear [20].¹

Heteroclinic Orbit in Rattleback Top. The rattleback phenomenon is a very interesting related problem in classical mechanics. A geometric form of the rattleback top is a truncated ellipsoid with an asymmetric mass distribution. Because of this asymmetric mass distribution and dissipation, the rattleback top spins stably about its short axis in one direction, and unstably in the other direction. When spun on a dry surface in the unstable direction, the rattleback top rocks about its intermediate axis and then reverses spin direction as shown in Fig. 6.2. Moreover, if set in a rocking motion about its intermediate or long axis, the rattleback top tends to spin in the stable direction. Some rattleback tops exhibit multiple spin-reversal which implies the existence of a heteroclinic orbit between saddle-like relative equilibria. Because of its asymmetry and dissipation, the rattleback top has no conserved quantity or known adiabatic invariant. For an exposition of what is known in this problem from the perspective of nonholonomic mechanics the reader is referred to [21; 40; 1].

Stochastic Resonance in Tippe Top. We conclude the paper with a conjecture. Stochastic resonance is a phenomenon that is ubiquitous in science

¹We thank Houman Owhadi (Caltech) for introducing us to this system.

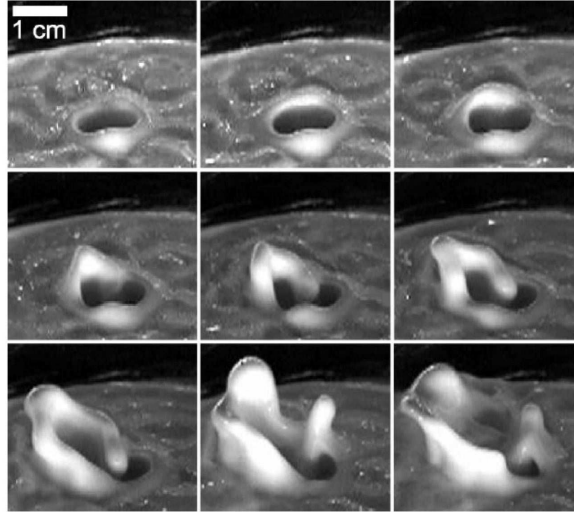


Figure 6.1: **Rising of Complex Fluids** [20]. Side view of the first steps toward the delocalized state in cornstarch. These photographs were taken every 0.9 s; time increases from left to right and top to bottom. An initial hump on the rim begins growing upward, reaches a maximum height, and then topples outward, enlarging the area of fluid motion. This process repeats until the entire surface of the liquid is active in the creation and destruction of vertical structures and voids (acceleration $a = 25g$, frequency $f = 80Hz$).



Figure 6.2: **Rattleback Top**. Sketch of the rattleback top initially spinning in the unstable direction, rocking back and forth, and then spinning in the opposite direction.

and engineering applications such as the ice ages, neurons, lasers, optical traps and quantum systems. In its basic form, it occurs in systems with stochastic forcing and a double-well potential whose depth changes periodically. If the period of the driving frequency matches the average noise-induced escape time from one well to the other, one obtains synchronized switching between two states of the system as shown in Fig. 6.3. Can such a phenomenon arise in the tippe top?

Examining theorem 4.1 it is clear there are parameter values where both inverted and noninverted states are Liapunov stable. This suggests that the effective potential the tippe top perceives in the $\xi_3^T \mathbf{e}_3$ direction is a double well. One can then let the magnitude of gravity change periodically and add structured stochastic forcing to realize stochastic resonance in the tippe top. The condition on the stochastic force is that it preserves the Jellett momentum

map. The tools for carrying out such an analysis: a Noether's theorem for stochastically forced and torqued mechanical systems, stochastically torqued rigid body equations, and ergodicity theorems, can be found in [9; 10; 11; 12].

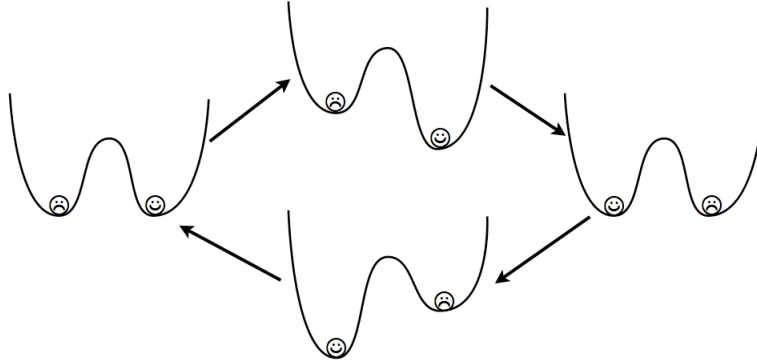


Figure 6.3: **Stochastic Resonance.** Stochastic resonance occurs in stochastically forced systems characterized by a double well potential that time-periodically changes depth. When the ratio of the mean-escape time from one well to another matches the driving frequency of the potential energy, then one obtains synchronized switching between two states of the system (e.g., inverted and noninverted states of the tippe top) which is depicted in the above cartoon by the happy and sad faces switching positions.

References

- [1] A. M. BLOCH, *Nonholonomic Mechanics and Control*, Interdisciplinary Applied Mathematics, Volume **24**, Springer-Verlag, (2003), 72-74.
- [2] A. M. BLOCH, P. S. KRISHNAPRASAD, J. E. MARSDEN, AND T. S. RATIU, *Dissipation induced instabilities*, Ann. Inst. H. Poincaré Anal. Non Linéaire, **11**, (1994), 37–90.
- [3] A. M. BLOCH, P. S. KRISHNAPRASAD, J. E. MARSDEN, AND T. S. RATIU, *The Euler–Poincaré equations and double bracket dissipation*, Comm. Math. Phys., **175**, (1996), 1–42.
- [4] A. M. BLOCH, J. E. MARSDEN, AND D. V. ZENKOV, *Nonholonomic dynamics*, Notices of the AMS, **52**, 302–329.
- [5] N. BOU-RABEE, J. E. MARSDEN, AND L. A. ROMERO, *Tippe Top Inversion as a Dissipation-Induced Instability*, SIAM J. Appl. Dyn. Syst., **3**, No. 3, (2004), 352–377.

- [6] N. BOU-RABEE, J. E. MARSDEN, AND L. A. ROMERO, *A geometric treatment of Jellett's egg*, *Z. Angew. Math. Mech.*, **85**, No. 9, (2005), 618–642.
- [7] N. BOU-RABEE, *Hamilton-Pontryagin Integrators on Lie Groups*, PhD Thesis, California Institute of Technology, 2007.
- [8] N. BOU-RABEE AND J. E. MARSDEN, *Hamilton-Pontryagin Integrators on Lie Groups: Introduction and Structure-Preserving Properties*, To appear in FOCM.
- [9] N. BOU-RABEE AND H. OWHADI, *Ballistic Transport at Uniform Temperature*, Submitted; arXiv:0710.1565.
- [10] N. BOU-RABEE AND H. OWHADI, *Ergodicity for Langevin Processes with Degenerate Diffusion in Momentums*, Submitted; arXiv:0710.4259.
- [11] N. BOU-RABEE AND H. OWHADI, *Stochastic Variational Partitioned Runge-Kutta Integrators for Constrained Systems*, Submitted; arXiv:0709.2222.
- [12] N. BOU-RABEE AND H. OWHADI, *Stochastic Variational Integrators*, Submitted; arXiv:0708.2187.
- [13] N. BOU-RABEE, L. A. ROMERO, AND A. G. SALINGER, *A multiparameter, numerical stability analysis of a standing cantilever conveying fluid*, *SIAM J. Appl. Dyn. Syst.*, **1**, (2002) 190–214.
- [14] N. G. CHETAYEV, *The Stability of Motion*, Permagon Press, 1961.
- [15] M. C. CIOCCI AND B. LANGEROCK, *Dynamics of the tippe top via Routhian reduction*, *Regular and Chaotic Dynamics*, **12**, 2007.
- [16] M. G. CLERC AND J. E. MARSDEN, *Dissipation-induced instabilities in an optical cavity laser: A mechanical analog near the 1:1 resonance*, *Phys. Rev. E*, **64**, (2001), 067603.
- [17] R. J. COHEN, *The tippe top revisited*, *Amer. J. Phys.*, **45**, (1) (1977), 12–17.
- [18] S. EBENFELD AND F. SCHECK, *A new analysis of the tippe top: Asymptotic states and Liapunov stability*, *Ann. Phys.*, **243**, (1995), 195–217.
- [19] F. R. GANTMACHER, *The Theory of Matrices*, Vol. II, Chelsea, New York, 1959.

- [20] D. I. GOLDMAN, E. C. RERICHA, F. S. MERKT, R. D. DEEGAN AND H. L. SWINNEY, *Persistent holes in a fluid*, Physical Review Letters, **92**, (2004), 184501 .
- [21] J. HERMANS, *Rolling Rigid Bodies with and without Symmetries*, PhD Thesis, University of Utrecht, 1995.
- [22] S. M. JALNAPURKAR AND J. E. MARSDEN, *Stabilization of Relative Equilibria II*, Regul. Chaotic Dyn., **3**, (1999), 161–179.
- [23] P. L. KAPITSA, *Dynamical Stability of a Pendulum when its Point of Suspension Vibrates*, In collected papers of P. L. Kapitsa, vol. II, Pergamon Press, (1965), 714–737.
- [24] R. KRECHETNIKOV AND J. E. MARSDEN, *On destabilizing effects of two fundamental non-conservative forces*, Physica D, **214**, (2006), 25–32.
- [25] R. KRECHETNIKOV AND J. E. MARSDEN, *Dissipation-Induced Instabilities in Finite Dimensions*, Rev. of Mod. Phys., **79**, (2007), 519–553.
- [26] J. E. MARSDEN, *Lectures on Mechanics*, Cambridge University Press, London, 174, 1992.
- [27] J. E. MARSDEN AND T. S. RATIU, *Introduction to Mechanics and Symmetry*, 2nd ed., Springer-Verlag, New York, 1999.
- [28] D. MERKIN, *Introduction to the Theory of Stability*, 2nd ed., Springer, New York, 1997.
- [29] T. MITSUI, K. AIHARA, C. TERAYAMA, H. KOBAYASHI, AND Y. SHIMOMURA, *Can a spinning egg really jump?*, Proceedings of the Royal Society A, **462**, (2006), 2897–2905.
- [30] H. K. MOFFATT AND Y. SHIMOMURA, *Classical dynamics: Spinning eggs—a paradox resolved*, Nature, **416**, (2002), 385–386.
- [31] H. K. MOFFATT, Y. SHIMOMURA, AND M. BRANICKI, *Dynamics of an Axisymmetric Body Spinning on a Horizontal Surface. Part I: Stability and the Gyroscopic Approximation*, Proceedings of the Royal Society A, **460**, (2004), 3643–3672.
- [32] H. K. MOFFATT, Y. SHIMOMURA, AND M. BRANICKI, *Dynamics of an Axisymmetric Body Spinning on a Horizontal Surface. Part II: Self-induced Jumping*, Proceedings of the Royal Society A, **461**, (2005), 1753–1774.

- [33] A. C. OR, *The dynamics of a tippe top*, SIAM J. Appl. Math., **54** (1994), 597–609.
- [34] W. PAUL, *Electromagnetic traps for charged and neutral particles*, Proc. from Int'l. School of Phys. Enrico Fermi, (1992), 419–517.
- [35] L. A. ROMERO, *Spin stabilized magnetic levitation of horizontal rotors*, SIAM J. Appl. Math. **63**, (2003), no. 6, 2176–2194.
- [36] L. A. ROMERO, *Passive levitation in alternating magnetic fields*, SIAM J. Appl. Math. **63**, (2003), no. 6, 2155–2175.
- [37] E. J. ROUTH, *The Advanced Part of a Treatise on the Dynamics of a System of Rigid Bodies*, Macmillan, New York, 1905.
- [38] W. THOMSON AND P. G. TAIT, *Treatise on Natural Philosophy*, Cambridge University Press, Cambridge, UK, 1879.
- [39] T. UEDA, K. SASAKI, S. WATANABE, *Motion of the Tippe Top: Gyroscopic Balance Condition and Stability*, SIAM J. Appl. Dyn. Syst., **4**, (2005), 1159–1194.
- [40] D. V. ZENKOV, A. M. BLOCH, AND J. E. MARSDEN, *The Energy-Momentum Method for the Stability of Nonholonomic Systems*, Dynamics and Stability of Systems, **13**, (1998), 123–166.